Solving fracture problems using an asymptotic numerical method

Loïc Daridon, Bertrand Wattrisse, André Chrysochoos, Michel Potier-Ferry

Solving fracture problems using an asymptotic numerical method

L. Daridon[1,3,*] , B. Wattrisse[1,3], A. Chrysochoos[1,3] and M. Potier-Ferry[2]

[1] LMGC – UMR 5508 ,UM2,CNRS, Université MONTPELLIER II CC 048, Place Eugène Bataillon, 34095 Montpellier cedex 5, France

[2] LPMM - UMR 7554, Université METZ, Ile du Saulcy, 57045 Metz cedex 01, France

[3] MIST laboratory, UM2,CNRS,IRSN.

Abstract

The present work deals with the use of asymptotic numerical methods (ANM) to manage crack onset and crack growth in the framework of Continuum Damage Mechanics (CDM). More specifically, an application of regularization techniques to a 1D cohesive model is proposed. The standard "triangle" damageable elastic model, often used in finite element codes to describe fracture of brittle materials, was chosen. Results associated with load-unload cycle showed that ANM is convenient to take numerically this specific non regular behaviour into account. Moreover, the present paper also shows that the chosen damageable interface model can be introduced in the generalized standard material formalism which unables us to define a complete energy balance associated with the damage process. In such a framework, the new damage state variable is a displacement. Finally, a 1D finite element application to a simple elastic damageable structure is shown to emphasize the potentialities of such an approach.

* Corresponding author – email : loic.daridon@univ-montp2.fr

1 Introduction

Asymptotic numerical methods (ANM) are based on the computation of a Taylor series expansion per step [1]. Because this is a high order computation technique, it is able to yield very accurate solutions, which is useful to follow highly non-linear response curves as for instance in unilateral contact or in the presence of bifurcations or quasi-bifurcations. Clearly crack propagation and damage mechanics lead to such very non-linear responses. So there is a need to adapt ANM in the case of damage mechanics and this is the subject of the present paper.

ANM has been widely applied to smooth partial differential equations such as non-linear elasticity [2, 3] and Newtonian fluid mechanics [4, 5]. It cannot be used directly for non smooth models such as unilateral contact, plasticity or damage, because the Taylor series exists only if the governing equations are defined by smooth functions. Nevertheless the non smooth constitutive equations can be regularised, as proposed in [6]. The study of anelastic problems by ANM has begun with deformation plasticity [7, 8]. Unilateral frictionless contact is the simplest example of non smooth mechanics and ANM has proved to be efficient in this case [9, 10]. Application of ANM for problems combining several strong non-linearities can be found in [11, 12]. The treatment of incremental plasticity is more difficult because there one has to manage two unilateral conditions, the first one to describe the elastic-plastic transition, the second for the elastic unloading. Corresponding regularization procedures have been proposed by Assidi et al [13] that permits to solve structural problems with elastic-plastic constitutive equations. A similar procedure could be applied in other cases, such as Coulomb friction law or damage mechanics, because these models combine also two different unilateral conditions, the first one in terms of stress and the second one in terms of strain rate, stress rate or of damage rate. In this paper we try to define a relevant ANM computational procedure for damage mechanics using cohesive zone

model (CZM) to predict crack propagation.

The subject of the present paper is the use of asymptotic numerical methods (ANM) to manage crack onset and crack growth in the framework of Continuum Damage Mechanics (CDM) with cohesive zone model. [14-16]. For the sake of simplicity, we limited hereafter our analysis to 1-D damageable interface. The interface model considered here is of a classical type, i.e. it relates load to normal displacement discontinuities. This type of model is often used to model initiation of composite delamination [17-19] or crack propagation using CZM. The chosen damageable interface law is the classical "triangle" damageable elastic model [20-22]. However, it must be noticed that extensions of such an analysis to multiaxial loadings and/or non-linear cohesive law [23, 24] can be considered using the same approach.

The paper is composed as follows: the constitutive equations of the chosen damageable elastic behaviour are presented in section 2. Their non-regular and regularized versions are successively shown. After a brief reminder of the numerical techniques associated with ANM approaches, various results are shown to underline the relevance and efficiency of the ANM predictions once an appropriate set of regularization parameters has been identified. Section 3 introduces a physically equivalent formulation of the chosen elastic damageable behavior compatible with generalized standard materials formalism [15-16]. The new formulation allows us to define a complete energy balance associated with the damage process. The mechanical equivalent of such a formulation change is then shown comparing results directly derived from the physical constitutive equations with those obtained using their thermomechanical version. Finally, Section 4 presents the results associated with interfacial crack propagation. The progressive degradation of a cohesive surface between two cantilever beams was considered, highlighting the interest of ANM approaches for simulating the ruin of engineering structures.

2 A smooth approximation for the cohesive model

As mentioned above, we limited hereafter our analysis to 1D linear (triangle) damage threshold. Figure 1 illustrates the classical triangular cohesive zone model (CZM) where f stands for the load applied to a material element while x symbolizes its elongation. The damage threshold can then be represented by a yield function:

$$g\left(f,x\right)=\left\langle f-(f_c-k_c x)\right\rangle^{+}=0\,, \tag{1}$$

where f_c and k_c are material constants. The elongation at rupture is then defined by $x_c = f_c/k_c$. The function $<.>^{+}$ stands for the positive part defined by $\left\langle A\right\rangle^{+}=\max\left(A,0\right)$. The accessible physical domain is defined by the negative values of the function $F=f-(f_c-k_c x)$ where $f\geq 0$. It implies that $H\left(F\left(f,x\right)\right)$=1 uniquely for the boundary values defined by $g\left(f,x\right)=0$

when H is the Heaviside function defined by:

$$\begin{cases} H\left(A\right)=1 & if \quad A\geq 0 \\ H\left(A\right)=0 & if \quad A<0 \end{cases}, \tag{2}$$

The elastic constitutive equation is then written as follow:

$$f=k_0\left(1-d\right)x \;\text{ for }\; F(f,x)\leq 0 \;\text{and}\; f\geq 0 \tag{3}$$

where d represents the damage variable classically defined over [0,1], 0 being associated with a virgin material element and 1 with a cracked element. Let us remind that the region where F would be positive, is not physically admissible. Equation 3 translates the elastic response of the

material, k_0 denoting the elastic stiffness of the virgin material. The damage only increases when the material state is on the threshold line ($F=0$) and remains on it ($\dot{F}=0$) with $\dot{x}>0$. The use of Eqs (1-3) allows then deriving the rate of damage by:

$$\dot{d}=\begin{cases} 0 & \text{if } F\left(f,x\right)<0 \text{ or } (F\left(f,x\right)=0 \text{ and } \dot{x}\le 0) \\ \dfrac{k_c x_c}{k_0 x^2}\dot{x}\,H\left(1-\dfrac{x}{x_c}\right) & \text{if } F\left(f,x\right)=0 \text{ and } \dot{x}>0 \end{cases} . \qquad (4)$$

Equation 4 can be simplified into a unique expression of $\dot{d}$ in order to simplify the regularization process:

$$\dot{d}=\frac{k_c x_c}{k_0}\frac{\langle\dot{x}\rangle^+}{x^2}H\left(1-\frac{x}{x_c}\right)H(F\left(f,x\right)) \text{ with } F\le 0 \qquad (5)$$

Where the positive part of $\dot{x}$ was introduced to ensure that damage does not occur during elastic unloading.

The constitutive equations can be grouped in the following system where the condition $F\left(f,x\right)\le 0$ was translated by $H\left(-F\left(f,x\right)\right)$:

$$\begin{cases} f=k_0\left(1-d\right)x & (a) \\ \dot{d}=\dfrac{k_c}{k_0}\dfrac{x_c\langle\dot{x}\rangle^+}{x^2}H\left(1-\dfrac{x}{x_c}\right)H\left(F\left(f,x\right)\right)H\left(-F\left(f,x\right)\right) & (b) \end{cases} \qquad (6)$$

Solving this system by using ANM just requires the regularization of the differential equation (6.b.).

2.1 Regularization procedure of the damage law

Computing a solution of the system (Eq 6) by using ANM requires the regularization of various

functions and operators. As in plasticity [3], specific regular functions $P_{\eta_0}^{+}(x)$, $H_{\eta_0}(x)$ and $\Pi_{\eta_0}(x)$ named respectively "positive part", Heaviside and "sampling" functions were introduced to regularize the operator $< . >^{+}$, the Heaviside function in the damage rate (Eq 6) and in the threshold function $g\left(f,x\right)$ (Eq 1) . These functions are defined by:

$$\begin{cases} P_{\eta_0}^{+}\left(x\right)=\dfrac{1}{2}\left(\sqrt{x^2+\eta_0}+x\right) \\ H_{\eta_0}\left(x\right)=\dfrac{1}{2}\left(1+\dfrac{x}{\sqrt{x^2+\eta_0}}\right) \\ \Pi_{\eta_1}\left(x\right)=\dfrac{\eta_0}{x^2+\eta_0}=4H_{\eta_0}\left(x\right)H_{\eta_0}\left(-x\right) \end{cases} \tag{7}$$

$\Pi_{\eta_0}(x)$ is the regularized version of a function which returns 1 for all values of the criterion $x=0$ and 0 if $x\neq 0$. The function $\Pi_{\eta_0}(x)$ composed with the threshold function $g\left(f,x\right)$ can be used instead of $H_{\eta_0}\left(F\left(f,x\right)\right)$ in the damage rate to take into account that $\left(f,x\right)$ is located upon the damage threshold. In Figure 2 the influence of the dimensionless regularization parameter η_0 on curves $\Pi_{\eta_0}(x)$, $H_{\eta_0}\left(x\right)$ and $P_{\eta_0}^{+}\left(x\right)$ is presented. We note in Figure 2(a) that for values of η_0=10^{-4} the solution is close to the Heaviside function . So by using Eqs (6-8), the following regularized expression of the damage rate can be proposed:

$$\dot{d}=\frac{k_c}{k_0}\frac{\dot{x}_0 P_{\eta_0}^{+}\left(\dfrac{\dot{x}}{\dot{x}_0}\right)}{x^2}x_c H_{\eta_0}\left(1-\frac{x}{x_c}\right)\Pi_{\eta_0}\left(F\left(f,x\right)\right) \tag{10}$$

The arbitrary parameter $\dot{x}_0$ is introduced to normalize the elongation rate, in order to use the same

dimensionless regularizing parameter for all functions (eq 10). In what follows displacement controlled test will be performed and $\dot{x}_0$ will be taken equal to the imposed elongation rate.

2.2 Computational techniques

This section focuses on the numerical implementation of Eq.(10) in the ANM framework. Considering the problem as a function of time and noting $U(t)=\begin{bmatrix} x(t) \\ d(t) \end{bmatrix}$, ANM proposes to develop the unknow *U(t)*, as a time power series:

$$U(t)-U_0=\sum_{n=1}^{N}(t-t_0)^n U_n \qquad (11)$$

where $U_0=\begin{bmatrix} x(t_0) \\ d(t_0) \end{bmatrix}$ and t_0 refers to the starting point of the current step. The truncation of the series is denoted by *N*. Recurrence formulae, that can be obtained in a standard way [3-6] yield the coefficients $U_n=\begin{bmatrix} x_n \\ d_n \end{bmatrix}$ of the series. There are now two strategies to solve the system Eq.(6) ; The first one is to develop in series *f* and *d*. The second one is to reduce system (6) to only one scalar equation by introducing the definition of *f(x)* (Eq 6a) into the equation defining $\dot{d}$. depending only on (*d*(*t*), *x*(*t*)) and to develop in series only *d*(*t*). We chose the second one. Classically, the length of a ANM step, denoted *R*, is defined automatically by a simple formula introduced in [5]:

$$R=\left(\varepsilon\frac{\|U_1\|}{\|U_N\|}\right)^{\frac{1}{N-1}} \qquad (12)$$

where ε is a small given number used to check the accuracy of the solution [1], ||.|| is a norm, for instance the Euclidian norm. To evaluate the performance of this method, first, we consider a simple loading-unloading tensile test. The material parameters used for the computational parameter study are $\{f_c = 1\,\mathrm{N.mm^{-1}},\ x_c = 1\,\mathrm{mm},\ k_0 = 1\,\mathrm{N.mm^{-2}}\}$. The ANM parameters are $\{N = 10,\ \varepsilon = 10^{-4}\}$.

2.3 Numerical results

All calculations presented hereafter were made using the formal computational code Maple®. In Figure 3, we present the influence of η_0 on the numerical step length defined in Eq 12, where each marker materializes the end of a computational step. It is worth noting that only the ten first steps were taken into account for each η_0 value in order to highlight a classical result of AMN which is an accumulation of steps at damage inception which correspond to stiff damage rate evolution. This has been already underlined in previous works dealing with other regularized problems [3, 8, 13]. The curves presented in Figures 4 to 6 are obtained for a displacement controlled test such as $x(t) = -at(t-1)\dot{x}_0$. In this numerical simulation, we use $\dot{x}_0 = 1\ \mathrm{mm}.s^{-1}$ and $a = 3\ s^{-1}$. The damage rate is evaluated by Eq.(10). Figures (4-6) present numerical results showing respectively the influence of the regularized parameter η_0 on the following responses: adimensional load, damage and damage rate with respect to adimensional elongation. Figure 4 shows the adimensional load-elongation diagram. Three stages can be easily pointed out: the linear elastic loading (i), the softening induced by damage growth (ii) and finally the elastic unloading (iii). The influence of η_0 is clearly observed on these curves small values of η_0 inducing a response close to the non-regularized behaviour. Figure 5 shows the associated damage responses for the same values of η_0. During stage (i) the damage increases all the less

since η_0 is low. During stage (ii) damage increases with respect to eq 10. During stage (iii), a damage steady state can be observed whatever the η_0 value. The trends observed in the previous figure are amplified in Figure 6 where the damage rate has been plotted. In particular the quasi perfect steady state evolution of the damage during elastic loading can be verified ($\dot{d} \cong 0 s^{-1}$).

3 A smooth approximation of cohesive model in the thermomechanical framework

Cohesive models describe the progressive degradation of material interfaces. The existence of irreversible deformation processes legitimates the use of thermodynamics and the introduction of intrinsic dissipation induced by the damage progress. We used the formalism of generalized standard materials (GSM) [15] to define a complete energy balance (1^{rst} principle of Thermodynamics) associated with the deformation process. Amounts of elastic and stored energy, intensity of dissipation and coupling heat sources predicted by the model will be allowed to be compared with experimental assessments as soon as they will be available. This confrontation should then lead to a strengthening of the model consistency [25- 27].

Hereafter the damageable elastic model described by Eq. (6) is resumed; a simplified form of the energy balance is chosen to make the thermomechanical model as close as possible to the previous mechanical one.

3.1 Hypotheses

Generally speaking the deformation energy spent during a mechanical loading involves energy dissipation, internal energy variation and heat induced by the thermomechanical coupling mechanisms [25]. In the case of the “triangle” damageable elastic interface behavior, we supposed that damage is a pure dissipative mechanisms and the only one. So the following hypotheses were considered;

(*i*) Deformation energy is either dissipated by damage mechanisms or elastically stored as long as a load can be applied.

(*ii*) All the thermomechanical coupling effects are neglected and namely the thermoelastic effects induced by thermal dilatation.

(*iii*) Only isothermal processes are considered. Consequently the thermodynamic potential does not take into account the heat stored or released and the dissipation potential does not consider irreversibility induced by heat diffusion. The energy dissipation is then only due to damage mechanisms.

3.2 Choice of state variables

Quite systematically, thermomechanical models dealing with damage consider d as a state variable. In this work, we proposed to swap d for its equivalent elongation variable x_{d} to simplify the writing of the yield function associated with the dissipation potential. The state variable set is then here (x, x_{d}).

Figure 1 shows that as soon as damage develops, $x = x_{\mathrm{d}}$ and $f = f_{\mathrm{d}}$ so that:

$$\begin{aligned} f_d &= (f_{\mathrm{c}} - k_{\mathrm{c}} x_{\mathrm{d}}) = k_{\mathrm{c}} \left(x_{\mathrm{c}} - x_{\mathrm{d}} \right) \\ &= k_0 (1-d) x_{\mathrm{d}} \end{aligned} \tag{12}$$

The equivalent elongation due to damage is then the bounded variable, x_{d}:

$$x_e = \frac{k_{\mathrm{c}}}{k_0 + k_{\mathrm{c}}} x_{\mathrm{c}} \le x_{\mathrm{d}} = \frac{k_{\mathrm{c}}}{k_0 (1-d) + k_{\mathrm{c}}} x_{\mathrm{c}} \le x_{\mathrm{c}} \tag{13}$$

3.3 State equations

According to the previous energy hypotheses and with the chosen set of state variables, the free energy is written as:

$$\psi(x,x_{\mathrm{d}}) = \frac{k_{\mathrm{c}}}{2}\left\langle x_{\mathrm{c}} - x_{\mathrm{d}} \right\rangle^{+} \frac{x^2}{x_{\mathrm{d}}}, \tag{14}$$

The following state equations can then be derived:

$$\begin{cases} f_{\mathrm{x}} = k_{\mathrm{c}} \left\langle x_{\mathrm{c}} - x_{\mathrm{d}} \right\rangle^{+} \dfrac{x}{x_{\mathrm{d}}} & \text{(a)} \\ f_{\mathrm{x_d}} = -\dfrac{k_{\mathrm{c}}}{2} x_c \left(\dfrac{x}{x_{\mathrm{d}}} \right)^2 H\left(x_c - x_d\right) & \text{(b)} \end{cases}, \tag{15}$$

The conjugated variables associated with x and x_{d} are respectively f_{x} and $f_{\mathrm{x_d}}$, f_{x} classically representing the reversible part of the load. It is worth noting that the free energy has been constructed so that this reversible part of the load equals the load itself, $f = f_{\mathrm{x}}$, in order to impose damage as the unique source of irreversibility, as decided before.

3.4 Evolution equation

Within GSM formalism, evolution laws are derived from the dissipation potential, a non negative convex function of the flux of state variables. After a Legendre-Fenchel transform, the dissipation potential becomes a dual function of the associated thermodynamic forces. When the behaviour requires the introduction of a threshold, (e.g. elastic domain, solid-solid transition diagram), a 3rd formulation, particularly convenient, is often adopted. This latter directly uses the threshold function and the normality rule to express the evolution equations. The irreversible part of the load vanishing here, the unique thermodynamic force is X_{d} such that $X_{\mathrm{d}} = -f_{x_{\mathrm{d}}}$ [16]. The triangle shape of the damage threshold can then be translated into a function G of X_{d} that reads:

$$G(X_{\mathrm{d}}) = X_{\mathrm{d}} - \frac{f_{\mathrm{c}}}{2} \leq 0, \tag{16}$$

The normality rule leads to:

$$\dot{x}_d = \begin{cases} 0 \ \text{ if } \ G < 0 & (a) \\ \lambda \dfrac{\mathrm{d}G}{\mathrm{d}X_\mathrm{d}} = \lambda,\ \lambda \geq 0 \ \text{ if } \ G(X_\mathrm{d}) = 0 & (b) \end{cases} \tag{17}$$

The Lagrange multiplier λ is strictly positive when damage develops, i.e. when the thermodynamic state is and remains on the threshold function. As expected, this can be written:

$$\dot{x}_d = \dot{x} \ \text{ if } \ G(X_\mathrm{d}) = 0 \text{ and } \dot{G}(X_\mathrm{d}) = 0 \tag{18}$$

Using the Heaviside function introduced in Eq.(5), the rate of x_d can be rewritten whatever the situation:

$$\dot{x}_d = \left\langle \dot{x} \right\rangle^+ H(G(X_\mathrm{d})) \tag{19}$$

3.5 Energy balance

Let us consider now an elongation-controlled loading. For the sake of simplicity we only consider loads starting from the virgin state (i.e. $x_\mathrm{d}(t=0) = x_\mathrm{e}$). At this point, two elementary cases can be considered:

Elastic loading: in this case, the elongation range x_max is less than x_e. No damage occurs, the dissipated energy remains equal to zero and the deformation energy is elastically stored:

$$x_\mathrm{max} \leq x_\mathrm{e} \quad w_\mathrm{def} = \int_0^{x_\mathrm{max}} f \,\mathrm{d}x = \frac{k_\mathrm{e}\, x_\mathrm{max}^2}{2} = w_\mathrm{e}(x_\mathrm{max}) \tag{20}$$

No dissipation occurring during the unloading from x_max to 0, the mechanical cycle is then a thermodynamic cycle.

Loading with damage: The maximal elongation x_max is now greater than x_e, as we consider the operating point on the damage threshold, we have $x_\mathrm{max} = x_\mathrm{d}$ then the energy balance can be written

as:

$$\begin{cases} x_{\max} > x_{\mathrm{e}} \qquad w_{\mathrm{def}} = w_{\mathrm{e}} + w_{\mathrm{d}} \\ w_{\mathrm{def}} = \int_0^{x_{\max}} f \,\mathrm{d}x = \dfrac{k_{\mathrm{c}}}{2}\left(\dfrac{k_{\mathrm{e}}\, x_{\mathrm{c}}^2}{k_{\mathrm{e}} + k_{\mathrm{c}}} - \left(x_{\mathrm{c}} - x_{\max}\right)^2 \right) \\ w_{\mathrm{e}} = \dfrac{1}{2} f_{\mathrm{d}} x_{\mathrm{d}} = \dfrac{k_{\mathrm{c}}}{2}\left(x_{\mathrm{c}} - x_{\max}\right) x_{\max} \\ w_{\mathrm{d}} = \int_{x_{\mathrm{e}}}^{x_{\max}} X_{\mathrm{d}} \,\mathrm{d}x_{\mathrm{d}} = \dfrac{f_{\mathrm{c}}}{2}\left(x_{\max} - x_{\mathrm{e}}\right) \end{cases} \tag{21}$$

The elastic energy being fully released during the unloading from $x_{\max}$ to 0, the deformation energy associated with the cycle is then completely dissipated and the loading cycle is no longer a thermodynamic cycle even if the free energy variation vanishes over such a cycle.

Figure (7) shows in the load elongation diagram, the areas corresponding to the different terms of the energy balance. Figure (8) presents the evolution of the energy balance until rupture.

3.6 Numerical results

As in the previous approach the elongation depends on time, it is natural to sight that the development parameter of the unknown, denoted *U(t)*, is the time, where $U(t) = \begin{bmatrix} x(t) \\ x_{\mathrm{d}}(t) \end{bmatrix}$. In this case all the unknowns are displacement. We perform, now, numerical simulation using equation 19 as elongation damage rate, equation 16 as damage threshold function and equation 15 as state laws. The curves presented Figures 9 to 12 are obtained for the same parameters and loading condition as the first study, namely an imposed displacement $x(t) = -3t(t-1)\dot{x}_0$. The material parameters used for the computational parameter study are $\{f_c = 1Nmm^{-1}, x_c = 1mm, k0 = 1Nmm^{-2}\}$. To determine the convergence radius of each step

we use equation eq 12 with $\varepsilon = 10^{-4}$. In this section we present the influence of η_0 on the thermodynamics quantities introduced previously.

First of all we present the influence of η_0 on the curve adimensional thermodynamic force $\frac{X_{\mathrm{d}}}{f_c}$ versus the adimensional elongation. We recall that the damage threshold is $\frac{X_{\mathrm{d}}}{f_c} = \frac{1}{2}$ It is clear on Figure 9 that more η_0 is small more the regularized threshold function is close to the theoretical one. This implies for large values of η_0, typically 10^{-2}, X_{d} increases as well before one is on the theoretical threshold (Figure 11) because $\dot{X}_{\mathrm{d}}$ is positive instead of null (Figure 12). In Figure 10, we observe that the chosen threshold function is the good one to obtain the triangular cohesive model. In this Figure (Figure 10) we notice the same influence of η_0 on the state variable f_x than those observed previously in figure 4, namely you need small value of η_0 to get a good agreement between the regularised problem and the real one. The main difference between the two approaches lies in the choice of state variables and threshold function you have to regularise.

4 Finite element formulation

We present here, a one-D finite element formulation of this cohesive zone model. The structure problem we study is a beam over a damageable elastic foundation defined in Figure 13. This type of modelling is used to study interfacial crack propagation in composite when there is no initial crack [28] or to study crack propagation in adhesive layer [29]. We use a classical Bernoulli displacement field associated with linear elasticity under the small strain hypothesis to describe the beam behaviour. We use the thermodynamic framework to describe the constitutive law of the foundation. Then, the variational formulation of the problem is based on the following total

potential energy:

$$P_{ot}(s,x_d) = -\int_0^L \frac{1}{2} EI\left(v''(s)\right)^2 ds - \int_0^L \frac{k_c}{2} \left\langle x_c - x_d(s) \right\rangle^+ \frac{v(s)^2}{x_d(s)} ds + Fv(L) \quad (22)$$

where s which belongs to [0,L] is the abscissa along the beam, $v(s)$ is the vertical displacement, E the Young modulus, I the quadratic moment, $\{k_c, x_c\}$ the characteristic of the damageable foundation and $x_d(x)$ the state variable previously introduce associated to its evolution law (Eq 18).

Let us now describe the ANM algorithm is the case of the monotonic loading. The weak formulation of the problem can be express by the following equations :

$$\begin{cases} \int_0^L EIv''(s)\delta v''(s) - k_c v(s)\delta v(s) ds + \int_0^L k_c ed(s) v(s) \delta v(s) ds = F(t)\delta v(L) \\ ed(s) = \dfrac{x_c}{x_d(s)} \\ wd(s) = \dfrac{v(s)}{x_d(s)} - 1 \\ td(s) = \left(wd(s)\right)^2 \\ \dot{x}_d(s) = \dot{v}(s) \dfrac{\eta_0}{td(s) + \eta_0} \end{cases} \quad (23)$$

The functions $\{ed(s), wd(s), td(s)\}$ are introduced to simplify equations. Following the ANM methodology, truncated Taylor series are introduced in (23).

$$\left\{\begin{array}{lll} x_d(s)=\sum_{k=0}^{N} xd_k(s)t^k & ; & v(s)=\sum_{k=0}^{N} v_k(s)t^k \\ ed(s)=\sum_{k=0}^{N} ed_k(s)t^k & ; & wd(s)=\sum_{k=0}^{N} wd_k(s)t^k \\ td(s)=\sum_{k=0}^{N} td_k(s)t^k & ; & F(t)=\sum_{k=0}^{N} F_k t^k \end{array}\right\} \tag{24}$$

The two last equations of Eq 23 can be rewritten as follow to simplify the introduction of truncated Taylor series in the non-linear problem to get linear problem at each order.

$$\left\{\begin{array}{l} ed(s)x_d(s)=x_c \\ \dot{x}_d(s)\left(td(s)+\eta_0\right)=\dot{v}(s)\eta_0 \end{array}\right. \tag{25}$$

This yields to N linear problems given by:

At the order 0 the initial solution verifies :

$$\left\{\begin{array}{c} \int_0^L EIv_0''(s)\delta v''(s)-k_c v_0(s)\delta v(s)ds+\int_0^L k_c\left(ed_0(s)v_0(s)\right)\delta v(s)ds=F_0\delta v(L) \\ ed_0(s)=\frac{x_c}{xd_0(s)} \\ xd_0(s)=\frac{k_c}{k_0+k_c}x_c \\ wd_0(s)=\frac{v_0(s)ed_0(s)}{xc}-1 \\ td_0(s)=wd_0(s)wd_0(s) \end{array}\right. \tag{27}$$

at the order 1 :

$$\begin{cases} \int_0^L EIv_1''(s)\delta v''(s) - k_c v_1(s)\delta v(s)ds + \int_0^L k_c\left(ed_0(s)v_1(s) + ed_1(s)v_0(s)\right)\delta v(s)ds = F_1\delta v(L) \\ ed_1(s) = -\dfrac{xd_1(s)ed_0(s)}{xd_0(s)} \\ xd_1(s) = \dfrac{v_1(s)\eta_0}{td_0 + \eta_0} \\ wd_1(s) = \dfrac{v_0(s)ed_1(s) + v_1(s)ed_0(s)}{x_c} \\ td_1(s) = 2wd_0(s)wd_1(s) \end{cases} \tag{28}$$

at the order k :

$$\begin{cases} \int_0^L EIv_k''(s)\delta v''(s) - k_c v_k(s)\delta v(s)ds + \int_0^L k_c\left(ed_0(s)v_k(s) + ed_k(s)v_0(s)\right)\delta v(s)ds = F_k\delta v(L) + F_k^{MAN} \\ ed_k(s) = -\dfrac{xd_k(s)ed_0(s)}{xd_0(s)} - \sum_{i=1}^{k-1}\dfrac{xd_{k-i}(s)ed_i(s)}{xd_0(s)} \\ xd_k(s) = \dfrac{v_k(s)\eta_0}{td_0 + \eta_0} - \sum_{i=1}^{k-1}(k-i)\dfrac{xd_{k-i}(s)td_i(s)}{xd_0(s)} \\ wd_k(s) = \sum_{i=0}^{k}\dfrac{ed_i(s)v_{k-i}(s)}{x_c} \\ td_k(s) = \sum_{i=0}^{k} wd_i(s)wd_{k-i}(s) \\ F_k^{MAN} = \int_0^L k_c\left(\sum_{i=1}^{k-1} ed_i(s)v_{k-i}(s)\right)\delta v(s)ds \end{cases} \tag{29}$$

4.1 Numerical results

We present here a numerical parametric study for a cantilever beam over a damageable foundation, defined on Figure 13. The geometrical parameters for the beam are: length L=0,3 m, width b=0,01 m and height h=0,02 m. The elastic parameters are: E= 200.10^9 Pa and ν=0,3. For the damageable foundation we used the following parameters: k_0=200 Pa, k_c=20 Pa, and x_c=0,05 m. The load applied at the end of the beam, x=L, is given by $F(t) = \dot{F}_0 t$ where $\dot{F}_0 = 10$ Ns^{-1}, the beam is clamped at x=0.

The ANM parameter used for studies presented in Figures 14 and 15 is $\varepsilon=10^{-4}$, on the presented curves each mark corresponds to the end of a step. Figure 14 presents the mesh influence on the convergence radius, when $\eta_0 = 5.10^{-3}$ and N=15. The increase of the number element induces a slight decrease of the convergence radius for the large radius (smooth nonlinearity), and the opposite for the zone where the nonlinearity is stiff (small radius). Figure 15 (a) and (b) show the influence of η_0 on the convergence radius, for a mesh with $n_{elem} = 15$. In figures 15 (a) and (b) the curves are respectively obtained for $N=10$ and $N = 20$. In the both cases, it is clear that, as in the 1D analysis, a decrease of η_0 induces a decrease of the convergence radius and an increase of N induces an increase of the convergence radius until the theoretical convergence radius is reach. So for a given value of the adimensional displacement at the beam edge, namely $V(L)/x_c = 1$, the number of steps needed to achieve this operating point varies from 9 ($N=20$ and $\eta_0 = 1.10^{-1}$) to 74 ($N=20$ and $\eta_0 = 1.10^{-3}$). Knowing that in a calculation step we calculate and build a tangent operator and N right-hand sides, the optimum time for a complete calculus will depend on relative time of the these two operations. Nevertheless the radius slightly increases for the first step because for small value of η_0 the occurrence of damage is delayed. In Figure 16, we point out the influence of the regularized parameter η_0

on the adimentional thermodynamical state variables $\frac{f_{x_d}}{f_c}$ and $\frac{f_x}{f_c}$ evaluated at x=L.

The regularization effect of η_0 clearly appears on these curves : the more η_0 is small the nearest of the real problem we are.

Figure 17 presents the distribution along the beam of $X_{d,}$ the thermodynamic force associated with x_d captured at the end of different loading steps. In the same way, Figure 18 shows the distributions of f_x . In Figure 19, we present the influence of the mesh density on x_d and $v(x),$ the vertical displacement of the neutral axis. We notice no localisation of the damage with an increase of numbers of element.

5 Conclusions.

We present in this paper an application of the ANM for the cohesive triangle zone model. We also propose a new thermodynamic formulation of this damageable model. This new formulation will facilitate the development of experimental studies regarding the thermodynamical effect that accompanies the damage process. We have implemented in a finite element code the developed model and performed a numerical simulation in the case of a cantilever beam over a non-linear elastic foundation. The obtained results for this 1-D modelling are encouraging. With the chosen material parameters for the interface, we observe that there is no

localisation of the damage with mesh resizing. In further development, we then propose to tackle the complete crack propagation problem with a FE implementation of the ANM based on Automatic Differentiation technique [30, 31].

6 References

[1] COCHELIN B., DAMIL N., POTIER-FERRY M., Méthode Asymptotique Numérique: une technique de résolution des équations non linéaires. Paris, London: Hermès Science Publishing, 2007.

[2] COCHELIN B., Méthode asymptotique-numérique pour le calcul non-linéaire géométrique. Habilitation à diriger les recherches. 1994

[3] COCHELIN B., DAMIL N., POTIER-FERRY M., Asymptotic-Numerical Method and Padé approximants for non-linear elastic structures , International Journal for Numerical Methods in Engineering, 37, p. 1187-1213, 1994.

[4] CADOU J.M., COCHELIN B., DAMIL N., POTIER-FERRY M., ANM for stationary Navier-Stokes equations and with Petrov-Galerkin formulation , International Journal for Numerical Methods in Engineering, 50, p. 825-845, 2001.

[5] MEDALE M., COCHELIN B., A parallel computer implementation of the Asymptotic Numerical Method to study thermal convection instabilities, Journal of Computational Physics, 228, p. 8249-8262, 2009.

[6] POTIER-FERRY M., DAMIL N., BRAIKAT B., DESCAMPS J., CADOU J.M., CAO H.L., ELHAGE-HUSSEIN A., Traitement des fortes non-linéarités par la méthode asymptotique numérique , Comptes rendus de l'Académie des Sciences, Paris, t. 324, Série II b, p. 171-177, 1997.

[7] BRAIKAT B., DAMIL N., POTIER-FERRY M., Méthodes asymptotiques numériques pour la plasticité , Revue européenne des éléments finis, 6, p. 337-357, 1997.

[8] ZAHROUNI H., POTIER-FERRY M., ELASMAR H., DAMIL N., Asymptotic Numerical Method for nonlinear constitutive laws , Revue Européenne des éléments finis, 7, p. 841-869, 1998.

[9] AGGOUNE W., ZAHROUNI H., POTIER-FERRY M., Asymptotic numerical methods for unilateral contact , International Journal for Numerical Methods in Engineering, 68, p. 605-631, 2006.

[10] ELHAGE-HUSSEIN A., POTIER-FERRY M., DAMIL N., A numerical continuation methodbased on Padé approximants , International Journal of Solids and Structures, 37, p. 6981-7001, 2000.

[11] BRUNELOT J., Simulation de la mise en forme à chaud par une méthode asymptotique numérique, Thèse de doctorat, Université de Metz, 1999.

[12] ABICHOU H., ZAHROUNI H., POTIER-FERRY M., Asymptotic numerical method for problems coupling several non-linearities , Computer Methods in Applied Mechanics and Engineering, 191, p. 5795-5810, 2002.

[13] ASSIDI M., DAMIL N., POTIER-FERRY M., ZAHROUNI H., Regularization and perturbation techniques to solve plasticity problems, International Journal of Material Forming, 2, p. 1-14, 2009

[14] PERALES F., BOURGEOIS S., CHRYSOCHOOS A., MONERIE Y. Two field multibody method for periodic homogenization in fracture mechanics of nonlinear heterogeneous materials, 75(11), p.3378-3398, 2008.

[15] HALPHEN B., NGUYEN QS., On generalized standards materials. Journal de mécanique. 14(1) , p. 39-63 1975.

[16] GERMAIN P., NGUYEN QS., SUQUET P. Continuum thermodynamics, Journal of applied mechanics-transaction of the ASME. 50 (4B):1010-1020, 1983.

[17] LADEVÈZE P., A damage computational method for composite structures. Computers and Structures 44 , p. 79–87 1992.

[18] CORIGLIANO A., ALLIX O., Some aspect of interlaminar dégradation in composites, International Journal of Solids and Structures. 38 (4) , p. 547-576, 2001.

[19] CORIGLIANO A., MARIANI S., Simulation of damage in composites by means of interface models: parameter identification. Composites Science and Technology. 61(15) , p. 2299-2315, 2001.

[20] DARIDON L., ZIDANI K. The stabilizing effects of fiber bridges on delamination cracks. Composites Science and Technology, 62(1) , p. 83 90, 2002.

[21] DARIDON L., COCHELIN B., POTIER-FERRY M. Delamination and fiber bridging modelling in composite samples. Journal of composite materials, 31(9) , p. 874-888, 1997

[22] ALFANO G. On the influence of the shape of the interface law on the application of cohesive-zone models. Composites Science and Technology, 66(6) , p. 723–730, 2006.

[23] MONERIE Y., RAOUS M. A model coupling adhesion to friction for the interaction between a crack and a fiber/matrix interface. Zeitschrift fur Angewandte Mathematik und Mechanik 80 p. 205–214 2000.

[24] CORIGLIANO A., RICCI M., Rate-dependent interface models : formulation and numerical applications. International Journal of Solids and Structures. 38, p. 547-576, 2001.

[25] CHRYSOCHOOS A. , HUON V., JOURDAN F., MURACCIOLE J.-M., PEYROUX R. , WATTRISSE B., Use of Full-Field Digital Image Correlation and Infrared Thermography Measurements for the Thermomechanical Analysis of Material Behavior, Strain. 46 , p. 117-130. 2010.

[26] BALANDRAUD X., CHRYSOCHOOS A., LECLERCQ S., PEYROUX R., Influence of the thermomechanical coupling on the propagation of a phase change front, Comptes rendus de l'académie des sciences serieII fascicule B-Mécanique. 329 (8) , p. 621-626, 2001.

[27] WATTRISSE B., MURACCIOLE JM., CHRYSOCHOOS A., Thermomechanical effects accompanying the localized necking of semi-crystalline polymers, International Journal of Thermal Sciences. 41 (5) , p. 422-427, 2002.

[28] TIAN Y., FU Y. , MAO Y., Nonlinear static/dynamic analysis for elasto-plastic laminated plates with interfacial damage evolution, Composite Structures, **93** (1),, p. 103-112, 2010

[29] HÖGBERG J.L., SØRENSEN B.F., STIGH U, Constitutive behaviour of mixed mode loaded adhesive layer, International Journal of Solids and Structures 44, p 8335–8354, 2007

[30] KOUTSAWA Y., CHARPENTIER I., DAYA EM., CHERKAOUI M. A generic approach for the solution of nonlinear residual equations. Part I : The Diamant toolbox. *Computer Methods in Applied Mechanics and Engineering*. 198 (3-4) , p. 572-577, 2008.

[31] BILASSE M., CHARPENTIER I., DAYA EM., KOUTSAWA Y. A generic approach for the solution of nonlinear residual equations. Part II : Homotopy and complex nonlinear eigenvalue method. *Computer Methods in Applied Mechanics and Engineering*. 198 (49-52) , p. 3999-4004, 2009.

7 Figures

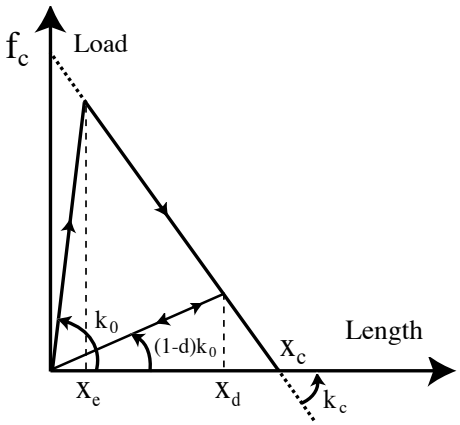

Figure 1: The "triangle" damageable elastic interface behaviour

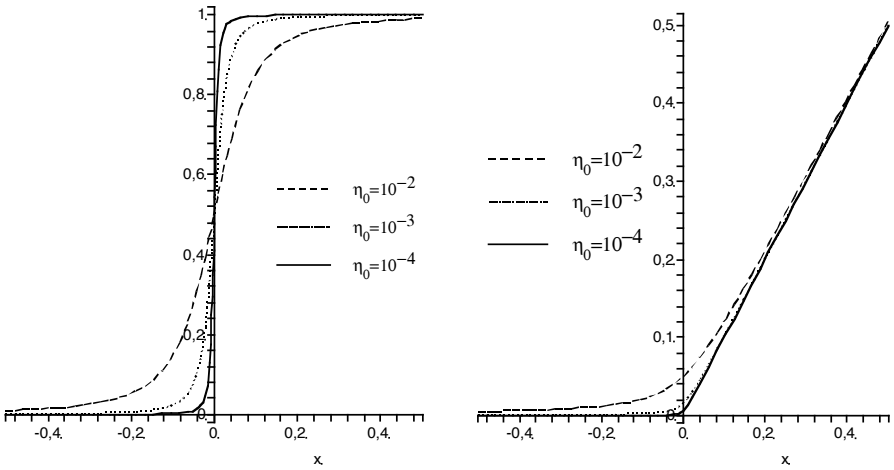

(a) $H_{\eta_0}\left(x\right)$ (b) $P^{+}_{\eta_0}\left(x\right)$

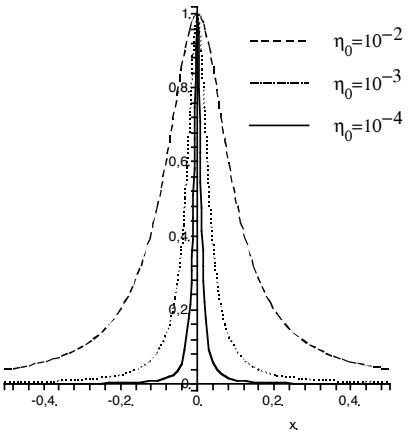

(c) $\Pi_{\eta_0}\left(x\right)$

Figure 2: Influence of η_0 on regularized functions

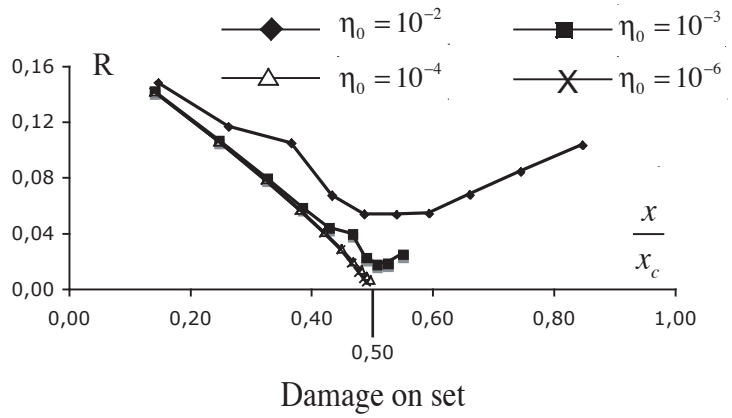

Figure 3: Influence of η_0 on the numerical step length

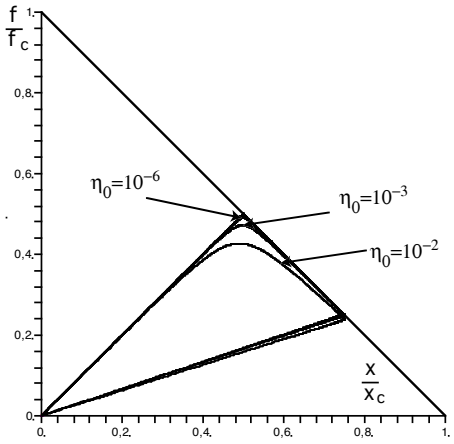

Figure 4: Influence of η_0 on loading curve

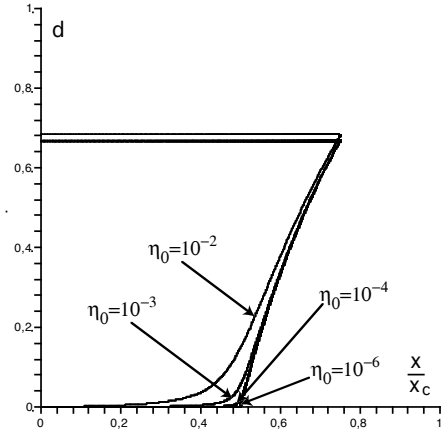

Figure 5: Influence of η_0 on damage variable

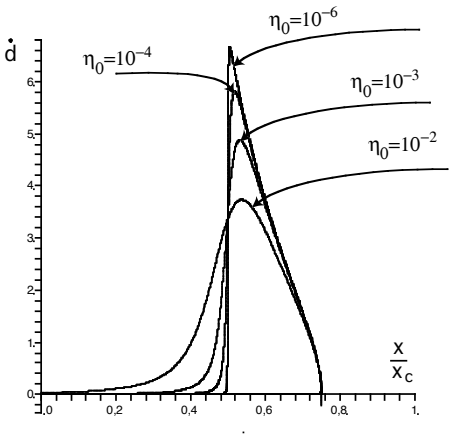

Figure 6 : Influence of η_0 on damage rate evolution

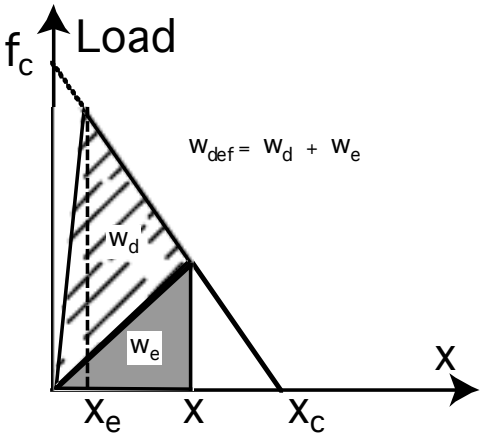

Figure 7 : Energy balance at elongation x

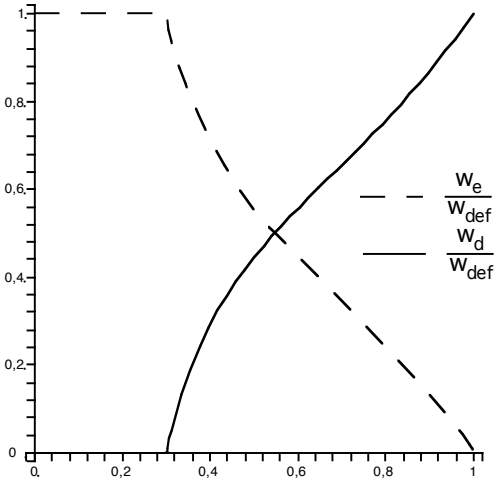

Figure 8 : Evolution of the energy balance

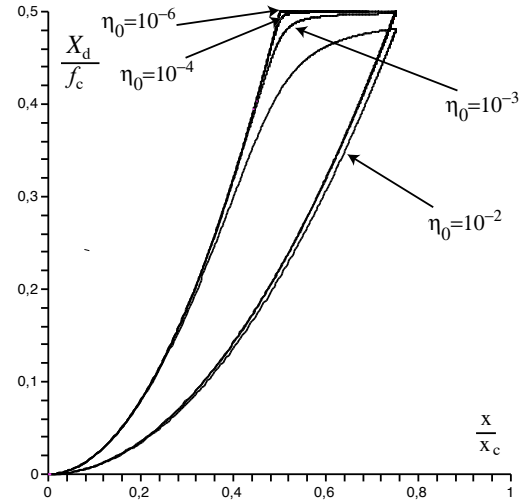

Figure 9: Influence of η_0 on X_d

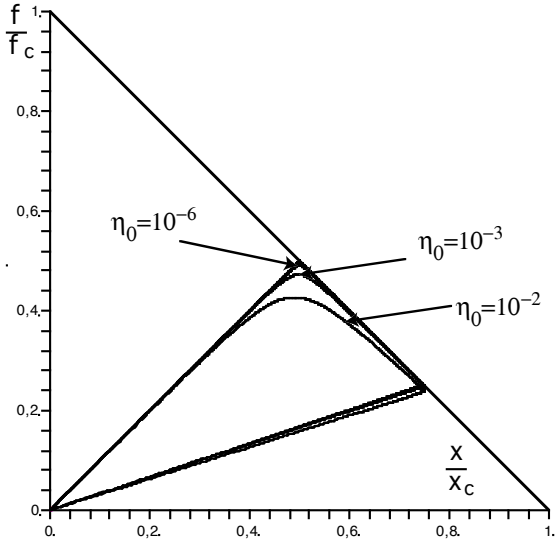

Figure 10 : Influence of η_0 on f_X

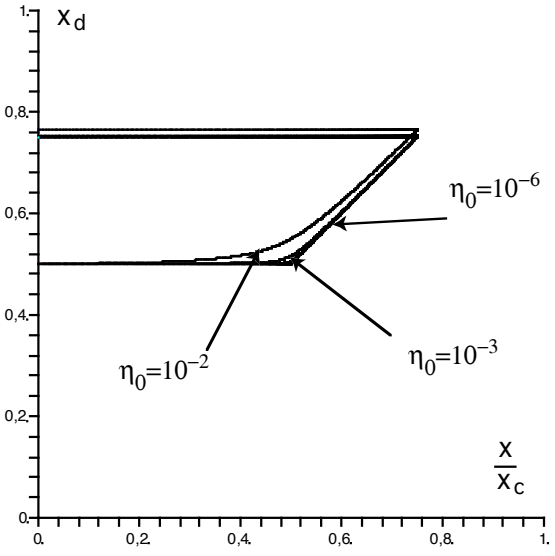

Figure 11: Influence of η_0 on state variable x_d

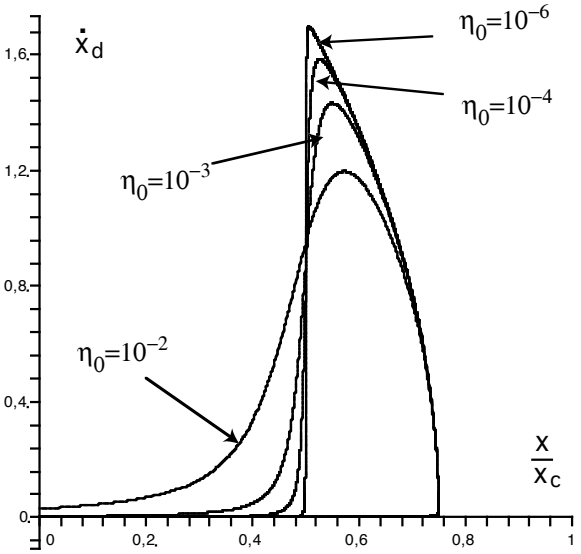

Figure 12: Influence of η_0 on $\dot{x}_d$

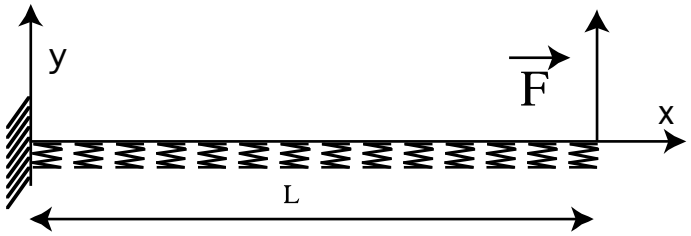

Figure 13 : Beam over damageable foundation

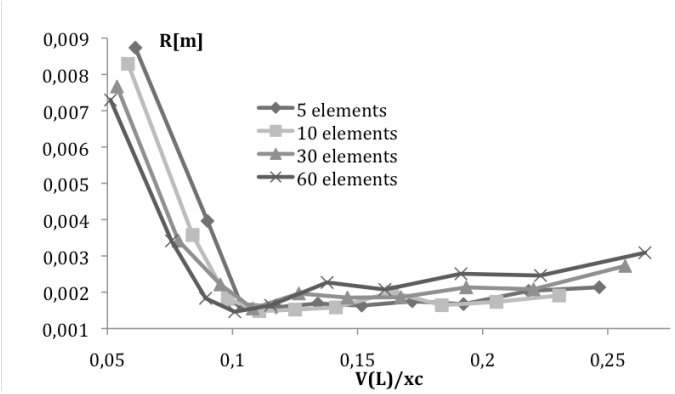

Figure 14: Mesh influence on convergence radius

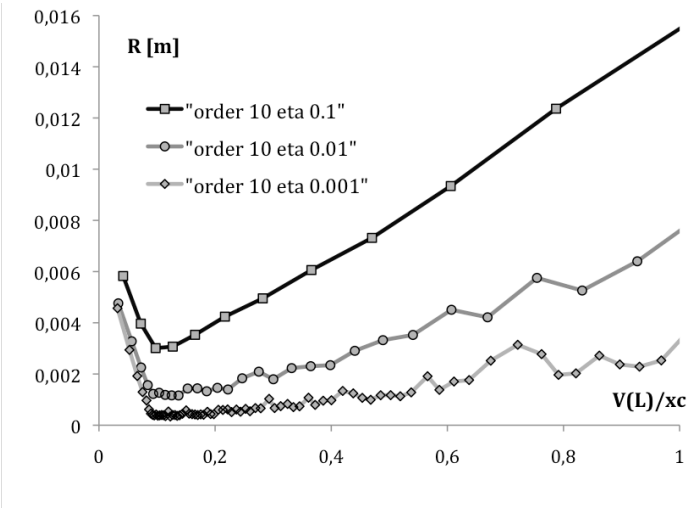

(a) N =10

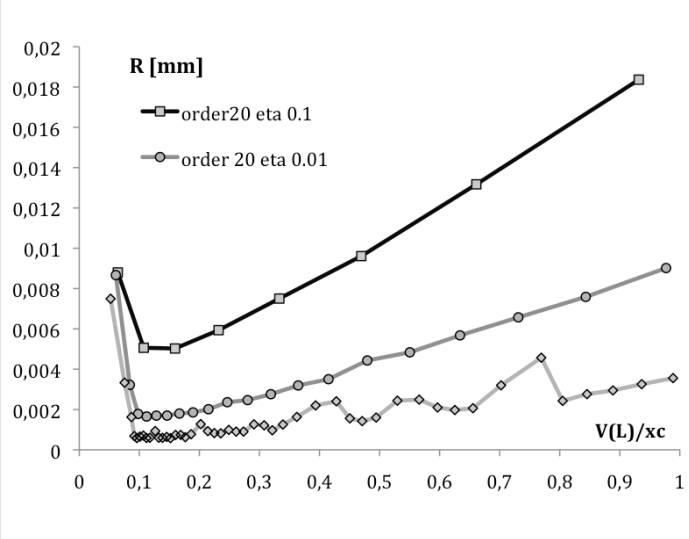

(b) N =20

Figure 15 : Influence of η_0 on convergence radius

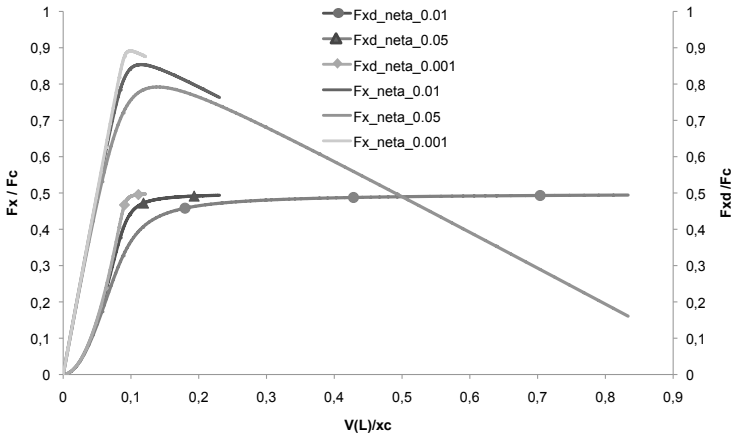

Figure 16 : Influence of η_0 on the thermodynamical state variables

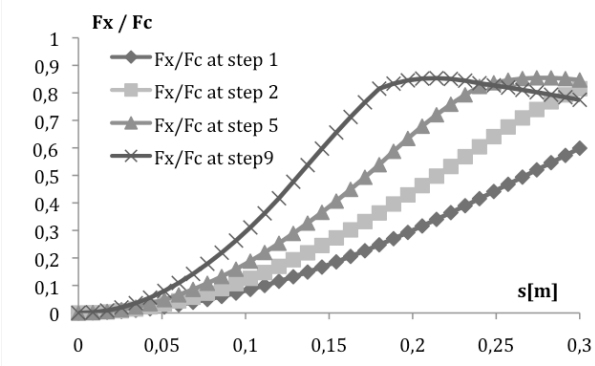

Figure 17 : Evolution of X_d along the beam

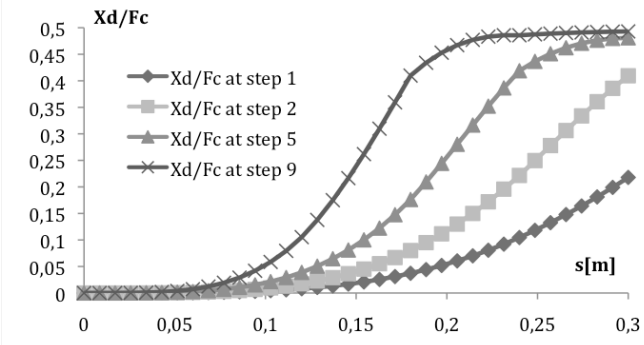

Figure 18 : Evolution of f_x along the beam

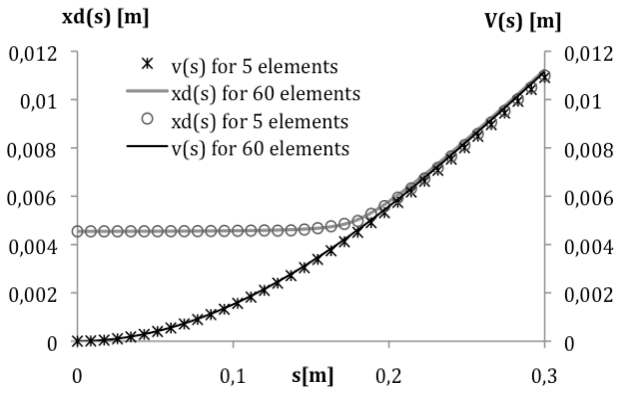

Figure 19 : Evolution of *v(s)* and $x_d(s)$ along the beam